Performance Analysis of Synchronous MC-CDMA in Mobile Rayleigh Channel With Both Delay and Doppler Spreads

Jean-Paul M. G. Linnartz, *Senior Member, IEEE*

***Abstract*—Rapid time variations of the mobile communication channel have a dramatic effect on the performance of multicarrier modulation. This paper models the Doppler spread and computes its effect on the bit error rate (BER) for multicarrier code division multiple access (MC-CDMA) transmission and compares it to orthogonal frequency division multiplexing (OFDM). Also, we evaluate the transmission capacity per subcarrier to quantify the potential of MC-CDMA and (coded-) OFDM. We focus on linear receivers, in particular those using the minimum mean-square error (MMSE) criterion. Our channel and system models allow the computation of analytical performance results. Simulations verify some commonly used, yet critical assumptions.**

***Index Terms*—Doppler effect, fading channels, intercarrier interference, multicarrier code division multiple access (MC-CDMA), multicarrier modulation, orthogonal frequency division multiplexing (OFDM), Rayleigh fading.**

I. Introduction

ORTHOGONAL frequency division multiplexing (OFDM) is a modulation method designed in the 1970s (see, e.g., [1]–[6]) in which multiple user symbols are transmitted in parallel using different subcarriers. Compared to other modulation methods, OFDM symbols have a relatively long time duration, but a narrow bandwidth. OFDM systems are designed such that each waveform is located around a particular subcarrier frequency and that the bandwidth is small enough to experience frequency-flat fading when received over a (moderately) frequency-selective channel. These subcarriers have overlapping sidelobes; nonetheless, the signal waveforms are designed to be orthogonal. A practical implementation involves an inverse (fast) Fourier transform (FFT) of the user bits before radio transmission. Due to the dispersive wireless channel, each subcarrier experiences a different attenuation and phase shift. The subcarriers remain orthogonal provided that the channel is time invariant. Of course, symbol errors are likely to occur on subcarriers, which are severely attenuated, so these are repaired by error correction codes. To this end, the redundancy in the error correction code is typically spread over many different subcarriers [5].

The OFDM receiver structure allows relatively straightforward signal processing to combat channel delay spreads, which was a prime motivation to use OFDM modulation methods in several standards, such as digital audio broadcasting (DAB) [3], [7], the digital terrestrial television broadcast (DTTB), which is part of the digital video broadcasting standard (DVB), and more recently the wireless local area network standard HIPERLAN II. In DAB, mobile reception leads to disadvantageous channel conditions, with both (frequency) dispersion and rapid variations of the channel with time. Reception of DTTB broadcast television "on the move" may not be seen as a major market today. Nonetheless, the DVB-DTTB system promises to become a high-speed delivery mechanism for mobile multimedia and Internet services. Tests have been conducted in summer 1999 offering mobile computing and web browsing over DTTB broadcast links with a GSM return channel [8]. This involves OFDM reception over channels with a Doppler spread and the corresponding time variations, which are known to corrupt the orthogonality of the OFDM subcarrier waveforms [2]. In such case, intercarrier interference (ICI) occurs because signal components from one subcarrier cause interference to neighboring subcarriers. In [9], the effect of ICI has been analyzed for a carrier frequency error and for Wiener phase noise. The performance of mobile propagation with Doppler spreads was addressed in [10], [11], and [33], [34].

This paper focuses on a code division multiple access (CDMA) type of transmission, which is an extension of the basic OFDM principle. In 1993, this form of multicarrier (MC) CDMA was proposed [12] and a similar system appears in [13], [14]. Several other multicarrier CDMA schemes have also been proposed [15], but we restrict our analysis to the one in [12]–[14]. Basically, it applies OFDM type of transmission to a multi-user synchronous direct sequence (DS)-CDMA signal. In conventional DS-CDMA, each user bit is transmitted in the form of many sequential chips, each of which is of short duration, thus having a wide bandwidth. In contrast to this, due to the FFT transform associated with OFDM, MC-CDMA chips are long in time duration, but narrow in bandwidth. Multiple chips are not sequential, but transmitted in parallel on different subcarriers. Here, we address the synchronous downlink. Our models apply to the case of a single broadcaster simultaneously sending data symbols over one MC-CDMA link,[1] as well as to the case of symbols from multiple users which are multiplexed onto a common multicarrier signal. We will use the term multi-user interference (MUI) for any mutual interference

Manuscript received February 15, 2000; revised October 18, 2000. This paper was presented in part at the *IEEE Conference on PIMRC'94*, The Hague, and the *IEEE Benelux Signal Processing Symposium*, SPS200, Hilvarenbeek, 2000.

The author is with Philips Research, Natuurkundig Laboratorium, WY 5656 AA Eindhoven, The Netherlands (e-mail: linnartz@ieee.org).

Publisher Item Identifier S 0018-9545(01)09842-5.

[1]Preferably such a scheme is called code division multiplexing, but we will use the more commonly used term (synchronous) CDMA.

between different symbols due to frequency dispersion of the channel, even though in the broadcast scenario all signals belong to the same user. The performance of MC-CDMA is an active areas of research, e.g., [12]–[14], [16], [20], [22], [24], [25], [29], [31] and the collection of papers in [6] and [32]. Since MC-CDMA uses OFDM, it is also vulnerable to rapid time variations of the channel. The effect of a carrier frequency offset in MC-CDMA was studied in [16]. We will extend this to Doppler spreads, we will address the MC-CDMA minimum mean-square error (MMSE) receiver, which hitherto only was discussed in conference publications and for slowly changing channels (e.g., [20], [22]) as the discussion of the merits of MC-CDMA versus straight OFDM or DS-CDMA is still ongoing, we will also address the capacity of the radio link from an information theoretic point of view.

The outline of the paper is as follows. Section II combines the OFDM transmit model with models for mobile Rayleigh multipath channels. It models the ICI under Doppler spreading. Section III uses this result to calculate the effect of a Doppler spread on the BER for a conventional OFDM receiver. Section IV addresses an MC-CDMA link, in particular one with a linear receiver for a channel with Doppler and delay spreads. The MMSE solution involves real time adaptive matrix inversion, but a simplification is proposed which mitigates the need for accurate channel estimation and adaptive filtering. Its performance is analyzed for reception with Doppler in Section V. Numerical and simulation results for OFDM and MC-CDMA are in Section VI. Channel capacity is evaluated in Section VII. Section VIII concludes this paper. New contributions are, among other things, an extension of the mathematical modeling for MC-CDMA (which not only allows better simulations, but also provides analytical results), inclusion of Doppler spreads, and an analysis of the "capacity" per subcarrier. It appears possible to express the performance of MC-CDMA over a Rayleigh channel in a "figure of merit" relative to the nondispersive additive white Gaussian noise (AWGN) linear time invariant (LTI) channel. In particular, we mathematically model the effect imperfect cancellation of MUI and the associated noise enhancements.

II. Formulation of the Model

Practical implementations of an OFDM transmission system use FFTs to create and decompose user data signals on multiple parallel subcarriers [5]. However, in our evaluation we adhere to a continuous-time representation, but we see no significant shortcoming in such analysis. We consider a transmit signal $s(t)$ of the multicarrier form

$$s(t) = \sum_{n=0}^{N-1} a_n \exp\{j\omega_c t + n\omega_s t\} \tag{1}$$

where

- ω_c carrier frequency;
- ω_s subcarrier spacing;
- n subcarrier number;
- N number of subcarriers;
- a_n modulation of the nth subcarrier carrying the user data.

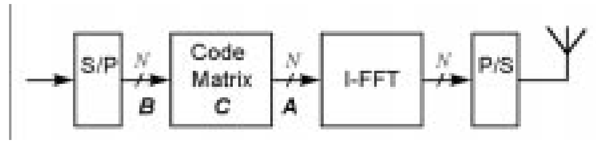

Fig. 1. Base-band equivalent representation of a generic OFDM and MC-CDMA transmit system.

As illustrated in Fig. 1, we use the following vector notation. For OFDM, vector $\boldsymbol{A}$ of length N carries a "frame" of user data, with $\boldsymbol{A} = [a_0, a_1, \ldots a_{N-1}]^T$, where the elements a_n are user symbols. In MC-CDMA, $\boldsymbol{A} = \boldsymbol{CB}$, where $\boldsymbol{C}$ is an N by N code matrix and $\boldsymbol{B} = [b_0, b_1, \ldots b_{N-1}]^T$ represents a frame of user data. We will refer to $\boldsymbol{B}$ as N user signals, without explicitly identifying whether or not all symbols come from the same end user. The kth column of $\boldsymbol{C}$ represents the "spreading code" of user data stream k, and will be denoted as $(c_k[0], \ldots c_k[N-1])^T$. A commonly used special case [12]–[14], which we will also consider here, is $\boldsymbol{C} = N^{-1/2}$ WH$_N$ where WH$_N$ is the Walsh–Hadamard matrix of size N by N. In that case, $\boldsymbol{C} = \boldsymbol{C}^{-1} = \boldsymbol{C}^H$, so $\boldsymbol{CC}^H = \boldsymbol{I}_N$ with $\boldsymbol{I}_N$ the N by N unit matrix. In another special case, namely that of $\boldsymbol{C} = \boldsymbol{I}_N$, the MC-CDMA system reduces to OFDM. For ease of analysis, we normalize the modulation as $Eb_i b_j^* = \delta_{ij}$, or equivalently $E\boldsymbol{BB}^H = I_N$. Then $E(\boldsymbol{AA}^H) = E\boldsymbol{C}(\boldsymbol{BB}^H)\boldsymbol{C}^H = \boldsymbol{CC}^H = I^H$. This implies that (in contrast to many studies for DS-CDMA) we address a "fully loaded" system, with $N-1$ interfering signals for a spread factor of N.

Fig. 1 illustrates such a transmitter. Frames are created by a serial-to-parallel (S/P) conversion of an incoming stream of data, applying the code spreading, an I-FFT, and a parallel-to-serial (P/S) conversion with prefix insertion. We will address the transmission of a single frame, and assume that interframe interference is avoided by choosing appropriate guard intervals. Hence, the elements of vectors $\boldsymbol{A}$ and $\boldsymbol{B}$ are constant with time. The frame duration, excluding any guard interval, is T_s, where $\omega_s T_s = 2\pi$.

The wide sense stationary uncorrelated scattering (WSSUS) multipath channel is modeled as a collection of I_w reflected waves. Each wave has its particular Doppler frequency offset ω_i, path delay T_i and amplitude D_i, each of which is assumed to be constant. That is, we make the common assumption that the time-varying nature of the channel arises from the accumulation of multiple components. Due to motion of the antenna at constant velocity, each component has a linearly increasing phase offset, though all with a different slope. The Doppler offset $\omega_i = 2\pi f_i$ lies within the Doppler spread $-2\pi f_\Delta \le \omega_i \le 2\pi f_\Delta$, with $f_\Delta = v f_c / c$ the maximum Doppler shift. Here, v is the velocity of the mobile antenna and c is the speed of light. The carrier frequency is $2\pi f_c = \omega_c$. The received signal $r(t)$ consists of the composition of all reflected waves, namely

$$r(t) = \sum_{n=0}^{N-1} \sum_{i=0}^{I_w-1} a_n D_i \exp\{j(\omega_c + n\omega_s + \omega_i) \times (t - T_i)\} + n(t). \tag{2}$$

Here, $n(t)$ represents AWGN. Detection of the signal at subcarrier m occurs by multiplication with the mth subcarrier frequency, thus with $\exp\{-j\omega_c t - jm\omega_s t + \varphi_m\}$ during an appropriately chosen interval T_s. A phase compensation $\varphi_m = 0$ is used.

Vector $\boldsymbol{Y}$ describes the outputs of the FFT at the receiver, with $\boldsymbol{Y} = [y_0, y_1, \ldots, y_{N-1}]^T$. Assuming rectangular pulses of duration T_s, after some resequencing of terms in the exponent we get

$$y_m = \sum_{n=0}^{N-1} \sum_{i=0}^{I_w-1} a_n D_i \int_0^{T_s} \exp\{j(n-m)\omega_s t + \omega_i t - j(\omega_c + n\omega_s + \omega_i)T_i\}\, dt + n_m. \quad (3)$$

Here n_m represents the noise sampled at the mth subcarrier. It can be shown to have variance $N_0 T_s$, with N_0 the spectral power density of the AWGN. We denote the subcarrier offset as $\Delta = n - m$, so

$$y_m = \sum_{n=0}^{N-1} \sum_{i=0}^{I_w-1} \frac{-ja_n D_i}{\Delta\omega_s + \omega_i}[\exp\{j(\Delta\omega_s + \omega_i)T_s\} - 1] \times \exp\{-j(\omega_c + \omega_i + n\omega_s)T_i\} + n_m. \quad (4)$$

We rewrite the above expression as $y_m = \sum_n a_n \beta_{m,n} T_s + n_m$ where $\beta_{m,n}$ can be interpreted as the "leakage" for a signal transmitted at subcarrier n and received at subcarrier m. Using $\mathrm{sinc}(x) = sin(\pi x)/\pi x$ and $\omega_s T_s = 2\pi$, we get

$$\beta_{m,n} = \sum_{i=0}^{I_w-1} \frac{D_i}{2} \mathrm{sinc}\left(n - m + \frac{\omega_i}{\omega_s}\right) \exp\{-j(\omega_c + \omega_i + \omega n_s)T_i - \frac{1}{2} j\omega_i T_s + j\pi(n-m)\}. \quad (5)$$

This result can be interpreted as sampling in frequency domain: the I_w multipath channel contributions appear weighed according to their individual Doppler offset ω_i. It confirms that due to the Doppler shifts, the detected signal y_m contains contributions from all n subcarrier signals, not only from $m = n$. All $\beta_{m,n}$s with $m \neq n$ lead to ICI, with amplitudes weighed by $\mathrm{sinc}(n - m + \omega_i/\omega_s)$.

A. Average ICI power

For a signal received at the mth output of the FFT, the covariance of the amplitude of the wanted component and the ICI is described by

$$\begin{aligned} &E_{\mathrm{ch}} \beta_{m,m-\Delta_1} \beta^*_{m,m-\Delta_2} \\ &= -1^{\Delta_1 - \Delta_2} E \sum_{i=0}^{I_w-1} \sum_{k=0}^{I_w-1} \frac{D_i}{2} \frac{D_k^*}{2} \mathrm{sinc}\left(\Delta_1 + \frac{f_i}{f_s}\right) \\ &\times \mathrm{sinc}\left(\Delta_2 + \frac{f_i}{f_s}\right) \exp\{-j(\Delta_1 - \Delta_2)\omega_s T_i\} \end{aligned}$$

where E_{ch} denotes the expectation over all channels. Clarke [18] and Aulin [19] studied a uniform probability density of the angle θ_i at which multipath waves arrive at the mobile [17], thus $f_\theta(\theta) = 1/(2\pi)$. The Doppler shift per wave equals $f_i = (v/c) f_c \cos(\theta_i)$, so

$$\theta = \arccos\left(\frac{c}{v}\frac{f_i}{f_c}\right) \quad \text{and} \quad \left|\frac{d\theta}{df}\right| = \frac{1}{\sqrt{f_\Delta^2 - f_i^2}}. \quad (6)$$

For an exponential delay spread and an omnidirectional antenna, this leads to the U-shaped spectrum [17]–[19] of the Doppler spread as follows:

$$\begin{aligned} &E_{\mathrm{ch}} \sum_{\substack{i: f < f_i < f + df; \\ T_i < \tau < T_i + dt}} D_i D_i^* \\ &= P_T [f_\theta(\theta) + f_\theta(-\theta)] \left|\frac{d\theta}{df}\right| f_\tau(\tau)\, d\tau \\ &= \frac{P_T}{2\pi T_{\mathrm{RMS}}} \frac{df}{\sqrt{f_\Delta^2 - f_i^2}} \exp\left\{-\frac{1}{T_{\mathrm{RMS}}}\right\} d\tau. \end{aligned} \quad (7)$$

Here, p_T is the local mean received power per subcarrier. We express the Doppler spread normalized to the subcarrier spacing as $\lambda = f_\Delta / f_s$. So

$$\begin{aligned} &E_{\mathrm{ch}} \beta_{m,m-\Delta_1} \beta^*_{m,m-\Delta_2} \\ &= -1^{\Delta_1 - \Delta_2} \frac{P_T}{2T_{\mathrm{RMS}}} \\ &\times \int_{-1}^{1} \frac{\mathrm{sinc}(\Delta_1 + x)\mathrm{sinc}(\Delta_2 + \lambda x)}{\sqrt{1 - x^2}}\, dx \\ &\times \int_0^{\infty} \exp\left\{-\left(\frac{1}{T_{\mathrm{RMS}}} + j(\Delta_1 - \Delta_2)_s\right)\tau\right\} d\tau \\ &E_{\mathrm{ch}} \beta_{m,m-\Delta_1} \beta^*_{m,m-\Delta_2} \\ &= \frac{P_T}{\pi} \int_{-1}^{1} \frac{\mathrm{sinc}(\Delta_1 + \lambda x)\mathrm{sinc}(\Delta_2 + \lambda x)}{\sqrt{1 - x^2}}\, dx \\ &\times \frac{-1^{\Delta_1 - \Delta_2}}{1 + j(\Delta_1 - \Delta_2)\omega_s T_{\mathrm{RMS}}}. \end{aligned} \quad (8)$$

The variance of the ICI signal leaking from transmit subcarrier $m - \Delta$ into received subcarrier m equals $P_\Delta = E_{\mathrm{ch}} \beta_{m,m-\Delta\beta^*_{m,m-\Delta}}$. Fig. 3 plots the received power P_0 and the ICI powers P_1, P_2 and P_3 versus the normalized Doppler spread λ for $p_T = 1$.

We further note that the strength of the amplitude of the wanted signal of the mth subcarrier has only a small correlation with the amount of ICI that it experiences. In fact, $E_{\mathrm{ch}} \beta_{m,m} \beta^*_{m,m-\Delta}$ is small because in good approximation $\mathrm{sinc}(\Delta + \varepsilon)$ is an even function for small ε and $\Delta = 0$ and an odd function of ε for integer $\Delta \neq 0$. Hence, the correlation coefficient ψ_Δ, between the wanted signal amplitude and unwanted ICI variance from the Δth subcarrier, defined as

$$\Psi_\Delta = \frac{E_{\mathrm{ch}} \beta_{m,m} \beta^*_{m,m-\Delta}}{\sqrt{E_{\mathrm{ch}} \beta_{m,m} \beta^*_{m,m} E_{\mathrm{ch}} \beta_{m,m-\Delta} \beta^*_{m,m-\Delta}}} \quad (9)$$

must be relatively small. Fig. 2 provides numerical values for the correlation Ψ_Δ for $\Delta = 1, 2,$ and 3.

III. Effect on BER for OFDM

Various definitions of BERs are relevant to a system designer: the instantaneous BER B_0 of an individual subcarrier with a given amplitude, and the local-mean BER B_1, thus averaged over all channels. We compute B_0 as the BER for a given $\beta_{n,n}$, but otherwise averaged over all channels, i.e., averaged over $\beta_{m,n} (m \neq n)$. So, B_0 can be interpreted as the expected value of

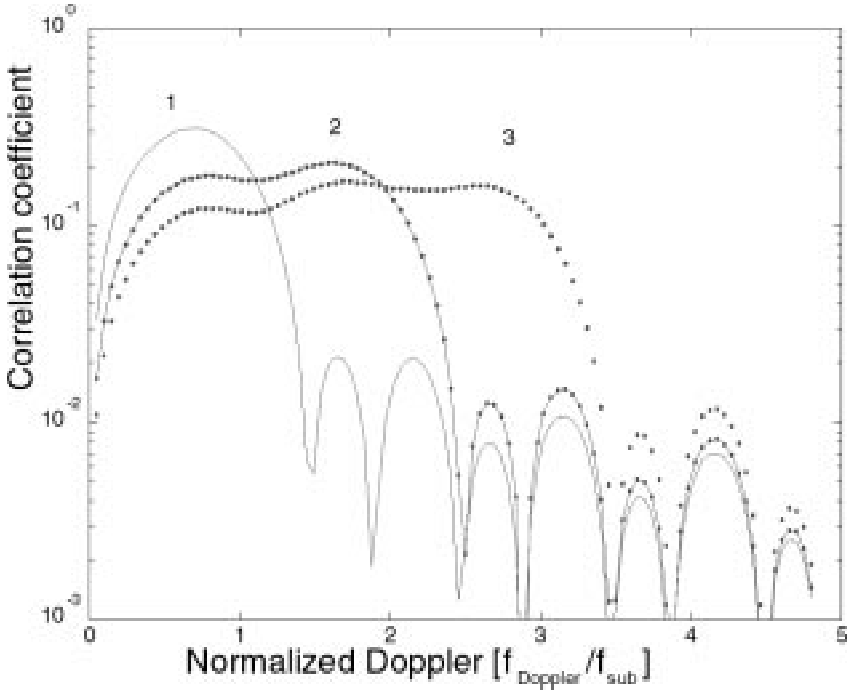

Fig. 2. Correlation coefficient between wanted signal and strength of the ICI.

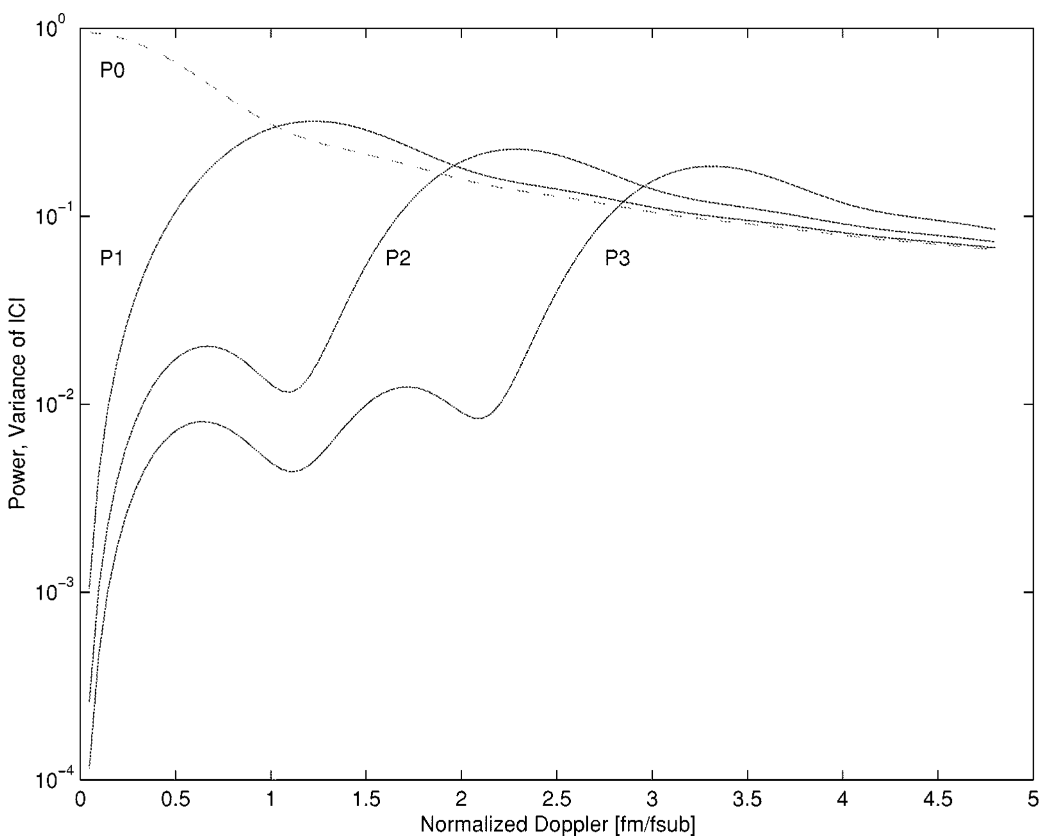

Fig. 3. Received power P_0 and the variances P_1, P_2 and P_2 of the ICI versus the normalized Doppler spread λ for $p_T = 1$.

the BER if only the subcarrier amplitude is known (or estimated) from measurements, but without any knowledge about the instantaneous value of the ICI. A typical OFDM receiver would forward such side information to the error correction decoder.

We consider a quasi-stationary radio link in which channel variations cause ICI, but the power $P_0 = \beta_{n,n}\beta_{n,n}^*/2$ for each subcarier is reasonably constant during an OFDM frame. Formally these two assumptions conflict, but for small Doppler shifts they may be reasonably accurate [10], [11]. For OFDM, the instantaneous signal-to-noise-plus ICI ratio γ equals

$$\gamma = \frac{\beta_{nn}\beta_{nn}^* T_s}{\sum_{\Delta \neq 0} P_\Delta T_s + N_0}. \tag{10}$$

We calculate BERs for BPSK, however the usual QAM can be expressed with similar formulas. In a Rayleigh channel, $\beta_{m,n}$ results from the addition of many independent waves, so it is a complex Gaussian random variable [17]. The contributions to the ICI become Gaussian, so the BER $B_0 = \text{erfc}(\sqrt{\gamma})$. Moreover, since $\beta_{n,n}$ is complex Gaussian, $\beta_{n,n}\beta_{n,n}^*$ has an exponential distribution with mean P_0. Therefore, the signal-to-noise ratio (SNR) γ has the probability density $f_\gamma(\gamma) = \gamma_{lm}^{-1} \exp\{-\gamma_{lm}^{-1}\gamma\}$ with local-mean SNR

$$\gamma_{lm} = P_0 T_s \bigg/ \left(N_0 + T_s \sum_{\Delta \neq 0} P_\Delta \right). \tag{11}$$

After averaging, the local-mean BER for BPSK modulation becomes

$$B_1 = \frac{1}{2} - \frac{1}{2}\sqrt{\frac{P_0 T_s}{\sum_\Delta P_\Delta T_s + N_0}}. \tag{12}$$

In the denominator, the summing is over all integer Δ within the range of active subcarriers, thus including $\Delta = 0$. Here we have implicitly assumed that the signal amplitude $\beta_{m,m}$ and the ICI $\beta_{m,n}(n \neq m)$ are statistically independent. Although the results in the previous section suggest that this is reasonable for our model (see (8), (9), and Fig. 2), we acknowledge that for other channel models this may not necessarily be an accurate assumption. Examples of situations where it may be inaccurate presumably include channels with a biased (nonuniform) angle of arrival, when the fading has a strong dominant component with nonzero Doppler shift or when the receiver has a significant frequency error.

The assumption of a uniformly distributed angle of arrival typically applies for long-term averages, whereas short-term channel modeling may require the use of a narrower angle spread.

For engineering applications with small Doppler spreads, a rule of thumb can be derived. We consider higher order tiers of neighboring subcarriers, but it appeared permissible to use a first-order approximation for the sinc. For arguments near zero, we take $\text{sinc}(f f_s^{-1}) \approx 1$, so we find that $P_0 \approx P_T$. For $\Delta = k$ (and for $f \ll f_s$), we approximate $\text{sinc}(k + f f_s^{-1}) \approx \text{sinc}(k) + (k + f f_s^{-1} - k)\text{sinc}'(k) = (-1)^k k^{-1} f f_s^{-1}$. Moreover, we observe that $P_k = P_{-k}$. Inserting these and using [21, eq. 2.272.3], we find

$$P_k \approx \frac{2P_T}{\pi f_\Delta k^2 f_s^2} \int_0^{f_\Delta} \frac{f^2\, df}{\sqrt{1 - f^2 f_\Delta^{-2}}} = \frac{f_\Delta^2 P_T}{\pi f_s^2 k^2}\left[\arcsin 1 - \sqrt{1 - \frac{f^2}{f_\Delta^2}}\right] \tag{13}$$

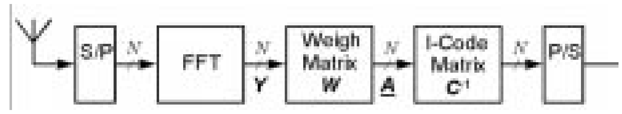

Fig. 4. Linear receiver architecture for MC-CDMA proposed in [12].

or $P_k = f_\Delta^2/(2 f_s^2 k^2) P_T$. We use that $\sum_{k=1} k^{-2} = \pi^2/6$. So, for BPSK OFDM and small λ

$$B_1 = \frac{1}{2} - \frac{1}{2}\sqrt{\frac{\gamma}{\frac{\pi^2 f_\Delta^2}{6 f_s^2}\gamma + 1}}. \tag{14}$$

IV. Linear Receiver Model for MC-CDMA

In MC-CDMA, after recovery of the subcarriers, the signals at the output of the FFT have to be "unspread" by applying the inverse code matrix. However, some weighing is needed to optimize performance and to mitigate the effects of the channel. At this point, we restrict ourselves to the class of (linear) receivers which make decisions based on linear combinations of all subcarrier signals, as, e.g., in Fig. 4. We explicitly introduce[2] the FFT, the inverse code matrix $\boldsymbol{C}^{-1}$, and a generic weigh matrix $\boldsymbol{W}$. This allows us to address a simple implementation for the receiver, where the weighing reduces to a simplified adaptive diagonal matrix, while the FFT and $\boldsymbol{C}^{-1}$ are nonadaptive, and can be implemented efficiently using standard butterfly topologies.

Two policies for the setting of the weigh matrix $\boldsymbol{W}$ with elements $w_{n,m}$ are intuitively appealing and have been proposed, e.g., in [12].

- If the receiver sets $w_{n,m} = \beta_{m,m}^* \delta_{nm}$, the system acts as a *maximum ratio combining* (MRC) diversity receiver. This receiver combines the subcarrier energy to minimize the SNR before the slicer. However, the multi-user interference is filtered out suboptimally. Only in a channel that is nonselective over the entire OFDM bandwidth, signals from other user bits remain orthogonal. If subcariers have different attenuation, the orthogonality of user signals is damaged, so MUI occurs. The MRC setting further worsens this effect.
- If the receiver sets $w_{n,m} = \delta_{nm}/\beta_{m,m}$ the system acts as an *zero-forcing equalizer*. This eliminates MUI because this receiver restores the orthogonality of the various user signals. It is equivelent to a decorrelating multi-user detector. A disadvantage of this setting is that noise enhancements are excessive.

A joint optimization can be derived from the following MMSE model [21]. As it provably outperforms MRC and equalization, we restrict the remainder of this paper to MMSE. It reduces the joint effects of noise, MUI and ICI. The MMSE estimate of the user data is equal to the conditional expectation $E\boldsymbol{B}\,|\,\boldsymbol{Y}$. We can rewrite this as

$$E\boldsymbol{B}\,|\,\boldsymbol{Y} = E\boldsymbol{C}^{-1}\boldsymbol{A}\,|\,\boldsymbol{Y} = \boldsymbol{C}^{-1}E\boldsymbol{A}\,|\,\boldsymbol{Y}. \tag{15}$$

[2]Mathematically, the receiver is equivalent to a single matrix operation, covering all three operations introduced here.

Here, the expectation E is over all instances of the modulation, while keeping the channel fixed. It shows that without loss of performance, one can estimate the modulation of each subcarrier as $\underline{\boldsymbol{A}}$ and then perform an inverse of the code matrix, using $\underline{\boldsymbol{B}} = \boldsymbol{C}^{-1}\underline{\boldsymbol{A}}$ for the user data. Let $\underline{\boldsymbol{A}}$ be a linear combination of $\boldsymbol{Y}$, namely $\underline{\boldsymbol{A}} = \boldsymbol{W}Y$. The optimum choice of matrix $\boldsymbol{W}$ follows from the orthogonality principle that the estimation error is uncorrelated with the received data, viz., $E(\boldsymbol{A}-\underline{\boldsymbol{A}})\boldsymbol{Y}^H = 0_N$ with 0_N an all-zero matrix of size N by N. Thus, we arrive at $\boldsymbol{W} = E[\boldsymbol{A}Y^H]\mathbf{R}_{\boldsymbol{Y}Y}^{-1}$, for the optimum estimation matrix. Here, $\boldsymbol{Y} = \boldsymbol{H}\boldsymbol{A} + \boldsymbol{N}$, where channel matrix $\boldsymbol{H}$ has the components $\boldsymbol{H}_{nm} = \beta_{nm}$. In such a case

$$\begin{aligned} E(\boldsymbol{A}\boldsymbol{Y}^H) &= E(\boldsymbol{A}(\boldsymbol{H}\boldsymbol{A})^H) + E(\boldsymbol{A}\boldsymbol{N}^H) \\ &= E\boldsymbol{A}\boldsymbol{A}^H\boldsymbol{H}^H = \boldsymbol{C}E\boldsymbol{B}\boldsymbol{B}^H\boldsymbol{C}^H\boldsymbol{H}^H = \boldsymbol{H}^H. \end{aligned} \tag{16}$$

Also, $\mathbf{R}_{YY}$, the covariance matrix of $\boldsymbol{Y}$ becomes

$$\begin{aligned} \mathbf{R}_{YY} &= E\boldsymbol{Y}\boldsymbol{Y}^H = \boldsymbol{H}E(\boldsymbol{A}\boldsymbol{A}^H)\boldsymbol{H}^H + E\boldsymbol{N}\boldsymbol{N}^H \\ &= \boldsymbol{H}\boldsymbol{H}^H + N_0T_s\boldsymbol{I}_N. \end{aligned} \tag{17}$$

Adaptive inversion of $\mathbf{R}_{YY}$ is needed to find the MMSE estimate of the signal in the presence of noise, MUI, and ICI. For simplicity, we initially review the special case of a channel without Doppler spread, thus, with $\boldsymbol{H} = T_s\mathrm{diag}(\beta_{0,0}, \ldots \beta_{N-1,N-1})$, as it was proposed in [21]. Then $E(\boldsymbol{A}Y^H)$ reduces to

$$E[\boldsymbol{A}Y^H] = \mathrm{diag}(\beta_{0,0}^*T_s, \beta_{1,1}^*T_s, \ldots, \beta_{N_{-1},N_{-1}}^*T_s) \tag{18}$$

and

$$\begin{aligned} \mathbf{R}_{YY} = \mathrm{diag}\big(&\beta_{0,0}\beta_{0,0}^*T_s^2 + N_0T_s, \beta_{1,1}\beta_{1,1}^*T_s^2 \\ &+ N_0T_s, \ldots, \beta_{N-1,N-1}\beta_{N-1,N-1}^*T_s^2 + N_0T_s\big). \end{aligned} \tag{19}$$

For this special case, we showed in [20] that $\boldsymbol{W}$ reduces to a diagonal matrix with elements

$$w_{n,m} = \frac{\delta_{n,m}\beta_{n,n}^*T_s^{-1}}{\beta_{n,n}\beta_{n,n}^* + \frac{N_0}{T_s}}. \tag{20}$$

That is, each subcarrier is weighed by a factor that depends only on the signal strength in that subcarrier and the noise; we interpret this as an automatic gain control and a phase corrector, which may operate independently for each subcarrier. The effect of adaptive (nonideal) tracking of subcarrier amplitudes in channels that are sufficiently slowly fading to avoid excessive Doppler was addressed in [22].

In the more general case of time-varying channels, implementation of this MMSE solution is quite involved because $\boldsymbol{W}$ does not reduce to a diagonal matrix. This implies that the optimum filter requires a (channel-adaptive) matrix inversion. Techniques have been studied to (blindly) estimate channel parameters in real time, e.g., [23], [24]. Mostly, such studies assume a limited number of (dominant) propagation paths (small I_w), so, in this respect, these differ from our Rayleigh model. In practice, it may not always be feasible or economic to estimate all $\beta_{m,n}$ accurately, invert the covariance matrix in real time, while adapting fast enough for the time variations of the channel, though research in this direction is progressing [28], [33], [34].

We propose a receiver that estimates only $\beta_{n,n}$, but no off-diagonal (ICI) terms $\beta_{m,n}$ with $m \neq n$. We take the weight settings of $\boldsymbol{W}$ to be as in (20), except that the noise N_0/T_s is replaced by the variance due to the joint contributions from noise and ICI. An MC-CDMA receiver that is designed for stationary reception, i.e., that is ignorant of ICI, would typically behave in this manner. In the next section, we calculate the BER. In the Appendix, we study the statistical behavior of $\beta_{n,n}$ and $w_{n,n}$ for Rayleigh channels with Doppler, in particular M_{ij} defined as $M_{ij} = E_{\mathrm{ch}}|\beta_{n,n}|^i|w_{n,n}|^j$. In contrast to most previous expressions in this section, the expectation is taken over all channels and denoted as E_{ch}. We exploit that $|\beta_{n,n}|$ is Rayleigh with mean-square value P_0.

V. Effect of BER for MC-CDMA

This section addresses the local-mean BER B_1. For MC-CDMA (but not for OFDM), the BER B_0 for one specific user signal converges to the local-mean BER if the number of subcarriers is sufficiently large and the transmit bandwidth largely exceeds the coherence bandwidth. In Section VI, simulations are used to verify the accuracy this approximation and to investigate the behavior for systems with fewer subcarriers. The decision variable for user bit zero, after combining all subcarrier signals, consists of

$$x = x_0 + x_{\mathrm{MUI}} + x_{\mathrm{ICI}} + x_n \tag{21}$$

where

- x_0 wanted signal;
- x_{MUI} multi-user interference (due to imperfect restoration of the subcarrier amplitudes);
- x_{ICI} intercarrier interference (due to crosstalk $\beta_{m,n}$ between a_n and y_m);
- x_{noise} noise.

- The wanted signal is

$$x_0 = b_0\frac{T_s}{N}\left[\sum_{n=0}^{N-1}\beta_{n,n}w_{n,n} + \sum_{m\neq 0}\sum_{n=0}^{N-1}\beta_{m,n}w_{n,n}c_0[n]c_0[n-m]\right]. \tag{22}$$

The expected value is

$$Ex_0 = b_0M_{11}T_s. \tag{23}$$

The variance of x_0 vanishes for large N, i.e., the system sees a nonfading channel.

- The contribution of the multi-user interference is

$$x_{\mathrm{MUI}} = T_s\sum_{k=1}^{N-1}b_k\left[\sum_{n=0}^{N-1}\beta_{n,n}w_{n,n}c_0[n]c_k[n]\right]. \tag{24}$$

The value of x_{MUI} depends on the choice of $\boldsymbol{C}$ and on the channel. For orthogonal spreading codes (i.e.,

$\Sigma_n c_0[n]c_k[n] = 0$) and a nondispersive channel (i.e., $\beta_{n,n}$ is constant with subcarrier frequency n), x_{MUI} can be made zero by taking $w_{n,m} = \delta_{n,m}$. For a dispersive channel, the orthogonality of spreading codes is eroded but the MUI level can remain low if the weight factors $w_{n,m}$ are appropriately chosen, as shown in a previous section. In such case, the variance of the MUI can be evaluated by observing that for any two orthogonal codes $c_j[n]$ and $c_k[n]$ with $j \neq k$, one can partition the set of subcarrier indixes n with $n = 0, 1, N-1$ into two sets, both with exactly $N/2$ elements, such that $A_- = \{n\colon c_j[n]c_k[n] = -1/N\}$ and $A_+ = \{n\colon c_j[n]c_k[n] = +1/N\}$ [24]. Here $A_+ \cup A_- = A$ ensures that $\Sigma_{A_+\cup A_-} c_j[n]c_k[n] = 0$. Hence

$$x_{\mathrm{MUI}} = \frac{T_s}{N}\sum_{k=1}^{N-1} b_k\left[\sum_{n\in A_+}\beta_{n,n}w_{n,n} - \sum_{n\in A_-}\beta_{n,n}w_{n,n}\right]. \tag{25}$$

Because of independence of user symbols and channel properties and mutual independence of user signals

$$\begin{aligned}\sigma^2_{\mathrm{MUI}} &= E_{\mathrm{ch}} E x_{\mathrm{MUI}} x^*_{\mathrm{MUI}} \\ &= \frac{T_s^2}{N^2} E\sum_{k=1}^{N-1} b_k^2 E_{\mathrm{ch}} \\ &\quad\times\left[\sum_{n\in A+}\beta_{n,n}w_{n,n} - \sum_{n\in A-}\beta_{n,n}w_{n,n}\right]^2 \\ \sigma^2_{\mathrm{MUI}} &= \frac{(N-1)T_s^2}{N^2}\left[E_{\mathrm{ch}}\left(\sum_{n\in A+}\beta_{n,n}w_n\right)^2\right. \\ &\quad + E_{\mathrm{ch}}\left(\sum_{n\in A-}\beta_{n,n}w_n\right)^2 - 2E_{\mathrm{ch}}\left(\sum_{n\in A+}\beta_{n,n}w_n\right) \\ &\quad\left.\times\left(\sum_{n\in A-}\beta_{n,n}w_n\right)\right].\end{aligned} \tag{26}$$

If we may assume that fading of the subcarriers is independent, we can write

$$\begin{aligned}E_{\mathrm{ch}}&\left(\sum_{n\in A+}\beta_{n,n}w_n\right)^2 \\ &= E_{\mathrm{ch}}\sum_{n\in A+}\sum_{m\in A+}\beta_{n,n}\beta_{m,m}w_{n,n}w_{m,m} \\ &= \frac{N}{2}E_{\mathrm{ch}}\beta_{n,n}^2 w_{n,n}^2 + \frac{N}{2}\left(\frac{N}{2}-1\right)(E_{\mathrm{ch}}\beta_{n,n}w_{n,n}) \\ &= \frac{N}{2}M_{22} + \frac{N}{2}\left(\frac{N}{2}-1\right)M_{11}^2\end{aligned} \tag{27}$$

and since $A_+ \cap A_- =$

$$E_{\mathrm{ch}}\left(\sum_{n\in A+}\beta_{nn}w_n\right)\left(\sum_{n\in A-}\beta_{nn}w_n\right) = \left(\frac{N}{2}\right)^2 M_{11}^2. \tag{28}$$

Thus

$$\sigma^2_{\mathrm{MUI}} = \frac{N-1}{N}T_s^2\left(M_{22} - M_{11}^2\right). \tag{29}$$

- The ICI contribution stems from crosstalk between subcarriers. Signal components which are present in $a_n = \Sigma_k c_k[n]b_k$ are spilled into $y_m = y_{n+\Delta}$, with strength $\beta_{n+\Delta,n}$. In the receiver, these are weighted by $w_{n+\Delta,n+\Delta}$ and unspread by $c_0[n+\Delta]$

$$\begin{aligned}x_{\mathrm{ICI}} &= T_s\sum_{n=0}^{N-1} a_n\sum_{\Delta\neq 0}\beta_{n+\Delta,n}w_{n+\Delta,n+\Delta}c_0[n+\Delta] \\ x_{\mathrm{ICI}} &= T_s\sum_{n=0}^{N-1}\sum_{k=0}^{N-1} b_k c_k[n] \\ &\quad\times\sum_{\Delta\neq 0}\beta_{n+\Delta,n}w_{n+\Delta,n+\Delta}c_0[n+\Delta].\end{aligned} \tag{30}$$

Inserting $a_n = \Sigma_k c_k[n]b_k$ and interchanging the sequence of the summings

$$\begin{aligned}x_{\mathrm{ICI}} = T_s\sum_{\Delta\neq 0}\sum_{n=0}^{N-1}\sum_{k=0}^{N-1} c_k[n]b_k\beta_{n+\Delta n} \\ \times w_{n+\Delta,n+\Delta}c_0[n+\Delta].\end{aligned} \tag{31}$$

Thus

$$\begin{aligned}\sigma^2_{\mathrm{ICI}} &= E_{\mathrm{ch}} E x_{\mathrm{ICI}} x^*_{\mathrm{ICI}} \\ &= T_s^2 E_{\mathrm{ch}} E\left[\sum_{m=1}^{N-1}\sum_{k=1}^{N-1} b_k\sum_{n=0}^{N-1}\beta_{mn}w_n c_0(n)c_k(n-m)\right]^2.\end{aligned} \tag{32}$$

The square of the triple sum simplifies because of $Eb_k b_j^* = \delta_{kj}$ and $E_{\mathrm{ch}}\beta_{i,j}\beta_{k,l} = \delta_{ij}\delta_{kl}$ and similar properties. We attribute no specific ICI reducing properties to the spreading code, i.e., we take $E[c_0[n]c_k[n-m]]^2 = N^{-2}$ and

$$\begin{aligned}\sigma^2_{\mathrm{ICI}} = \frac{1}{N}E\sum_{k=1}^{N-1} b_k^2 E&\left[\sum_{\Delta\neq 0}[c_0(n)c_k(n-m)]^2\right. \\ &\left.\times E_{\mathrm{ch}}\sum_{n=0}^{N-1}|\beta_{m,n}|^2 E_{\mathrm{ch}}\sum_{n=0}^{N-1}|w_{n,n}|^2\right].\end{aligned} \tag{33}$$

Thus

$$\sigma^2_{\mathrm{ICI}} = \Sigma_{\Delta\neq 0}p_\Delta M_{02}T_s^2. \tag{34}$$

Here, the question arises whether a system designer can chose the spreading matrix $\boldsymbol{C}$ such that the ICI is mitigated below the level expressed by (34). Such effort requires the cross-correlation $\Sigma_n c_0[n]c_k[n-m]$ to be small. This problem seems to be the time-frequency dual of the well-known problem of finding good codes for asynchronous

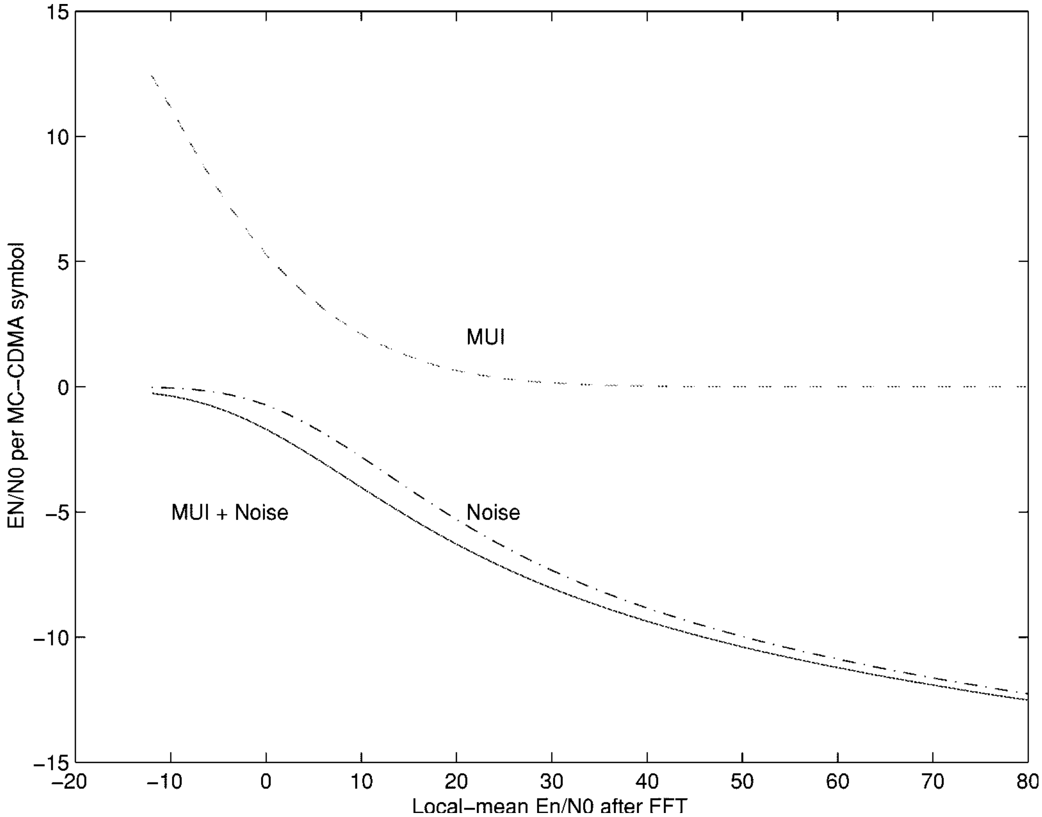

Fig. 5. MC-CDMA figure of merit ζ in decibels versus the local-mean SNR on Rayleigh channel.

DS-CDMA with good cross *and* autocorrelation properties to combat delay spread. Walsh–Hadamard codes have no particular properties to achieve good autocorrelation properties and their autocorrelation behavior can be approximated by the behavior of randomly chosen codes. Here, the situation here more involved because each term $c_0[n]c_k[n-m]$ is multiplied by $\beta_{m,n}$ and $w_{n,n}$, which are complex valued with random mutually independent arguments. Thus, even if the code had good autocorrelation properties, the channel delay spread erodes the attenuation of the ICI hoped for.

- The variance of the noise collected over all subcarriers weighted by $w_{n,n}$ becomes

$$\sigma_{\text{noise}}^2 = NM_{02}N_0T_s. \quad (35)$$

Since we consider ensembles of many different channels, $x_{\text{MUI}}, x_{\text{ICI}}$ and x_{noise} are zero-mean complex Gaussian. So, the local-mean BER for BPSK becomes $B_1 = (1/2)\,\text{erfc}\sqrt{E_N/N_0}$ with

$$\frac{E_N}{N_0} = \frac{M_{11}^2T_s^2}{\sigma_{\text{ICI}}^2 + \sigma_{\text{MUI}}^2 + \sigma_{\text{noise}}^2} = \frac{M_{11}^2}{(M_{22} - M_{11}^2) + M_{02}\left[\sum_{\Delta\neq 0} p_\Delta + \frac{N_0}{T_s}\right]}. \quad (36)$$

Because of the mathematical structure of this result, we can introduce the figure of merit ζ and rewrite (36) as $E_N/N_0 = \zeta P_0T_s/N_0$. Thus, ζ is a system parameter, which gives the improvement of MC-CDMA in a Rayleigh *fading* channel over narrow-band transmission in a *nonfading* channel. For very poor local-mean SNRs (large P_0T_s/N_0), the noise largely dominates over the MUI and the MC-CDMA MMSE receiver acts mainly as a maximum ratio combiner. Since $w_{n,n} \cong \beta_{n,n}/N_0$

$$M_{11} \to E\beta_{n,n}^2/N_0 = P_0/N_0$$
$$M_{02} \to E\beta_{n,n}^2/N_0^2 = P_0/N_0^2$$
$$M_{22} \to E\beta_{n,n}^4/N_0^2 = 2P_0^2/N_0^2$$

and ζ tends to unity (0 dB).

VI. Numerical and Simulation Results

As is seen from the BER expression and (36), the MMSE cancellation of the MUI leads to a noise penalty. Two terms occur in the denominator, one is due to imperfect cancellation of MUI, the other one is due to noise. The ICI is not actively cancelled, and contributes to the BER. Fig. 5 plots ζ and also the individual effects from MUI and noise, relative to the SNR per subcarrier. That is, it plots $(M_{11}/(M_{22} - M_{11}^2))/(P_TT_s/N_0)$ and $(M_{11}T_s/M_{02}N_0)/(P_TT_s/N_0)$. It is seen that the noise penalty increases monotonically with the local-mean SNR.

Fig. 6 plots the local-mean BER for BPSK versus the SNR in a very slowly changing Rayleigh-fading channel without Doppler spread and ICI ($v = 0$). Curves (AWGN), (OFDM) and (3—MC-CDMA) are theoretical results. Curve (AWGN) depicts the BER of BPSK in a channel without fading, using $\text{erfc}\sqrt{(E_N/N_0)}$. Curve (OFDM) gives the BER for a narrow-band Rayleigh-fading channel ($N = 1$), which is

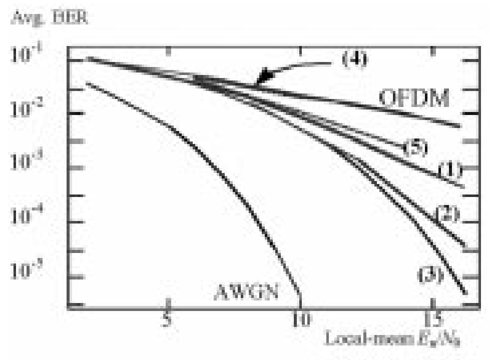

Fig. 6. Local mean average BER versus SNR. Theory: (3, AWGN, OFDM) and simulations (1, 2, 4, 5). (“AWGN”): BPSK, no fading, AWGN (“OFDM”): (1) $N = 8$, uncorrelated fading. (2) $N = 8$, highly correlated fading. (3) Infinitely many subcarriers. (4) $N = 8$, highly correlated fading. (5) $N = 8$, lightly correlated fading.

the same as the local-mean BER for OFDM, before any error correction. Moreover, it models MC-CDMA with $N = 1$. Curve (3) is the local-mean BER for MC-CDMA for $N \to \infty$. Curve (1) and (2) are Monte Carlo simulations for a system with N is 8 and 64 subcarriers, respectively. Curves (4) and (5) for correlated Rayleigh fading have been simulated in the frequency domain. All subcarrier amplitudes are known to be zero-mean complex Gaussian with covariance matrix Γ [17]–[19]

$$\Gamma = \begin{bmatrix} \chi_{00} & \chi_{10} & \cdots & \chi_{N0} \\ \chi_{01} & \chi_{11} & \cdots & \chi_{N1} \\ \cdots & \cdots & \cdots & \cdots \\ \chi_{0N} & \chi_{1N} & \cdots & \chi_{NN} \end{bmatrix} \tag{37}$$

with

$$\chi_{nm} = E\beta_{n,n}\beta_{m,m} = \frac{1}{1 + 2\pi j(n-m)T_{\text{rms}}/T_s} \tag{38}$$

where T_{RMS} is the delay spread of the radio channel. In a Monte Carlo simulation, we generated channels from an independent identically distributed (i.i.d.) vector of complex Gaussian random variables $\boldsymbol{G}$, with unity variance and length N. This vector was then multiplied by an $N \times N$ matrix $\boldsymbol{A}$, such that $\boldsymbol{A}A^H = \Gamma$, to create $\text{diag}(\boldsymbol{H}) = [\beta_{0,0}\beta_{1,1}, \ldots, \beta_{n,n}] = \boldsymbol{A}\boldsymbol{G}$, and $\beta_{m,n} = 0$ for $n \neq m$ (no Doppler). Then, the weight vector $\text{diag}(\boldsymbol{W})$ was determined from $\text{diag}(\boldsymbol{H})$ using (20). This results in amplitudes for the wanted signal (x_0), amplitudes for the MUI, and a noise amplification term so the BER for this particular channel can be calculated. Average BERs have been obtained by repeating this process for different channels $\boldsymbol{G}$.

The average BER versus the SNR for correlated fading was also simulated for the case of $N = 8$ with $T_{\text{RMS}}/T_s = 0.001$ and 0.125 in curve (4) and (5), respectively. Results show that the assumption of i.i.d. fading at the subcarriers is optimistic. The differences amoung the curves (3) and those for finite N are due to the fact that the SNR after despreading still contains fading. The slope of the curve for large SNR is determined mainly by the degree of diversity, say the “resolvable” number of independently fading channel components, which is roughly equal to $\min(N, T_{\text{RMS}}/T_s + 1)$. For instance, curve (4) addresses the case that all subcarriers exhibit highly correlated fading ($T_{\text{RMS}}/T_s = 0.001$), then the BER is very close to that of a single flat-fading channel ($N = 1$, curve OFDM).

The effect of Doppler spreading at 4 GHz is introduced in Fig. 7. Here, we consider a system with (infinitely) many subcarriers. We inserted typical values for DTTB but consider MC-CDMA instead of the standardized OFDM. The frame duration is $T_s = 896$ microseconds, with an FFT size of $N = 8192$. This corresponds to a subcarrier spacing of $f_s = 1.17$ kHz and a data rate of 9.14 Msymbols/s. Fig. 7 shows the local mean BER versus antenna speeds v for E_b/N_0 of 10, 20, and 30 dB. MC-CDMA appears to largely outperform uncoded OFDM.

VII. Channel Capacity

Comparison between the BER for of MC-CDMA and *uncoded* OFDM is unfair in the sense that OFDM can exploit channel state information about fading subcarriers in its error correction decoder. In a MC-CDMA downlink, any user symbol is spread over all subcarriers. After despreading from many subcarriers, all symbols see a relatively fixed, nonfading channel. It is beyond the intentions of this paper to exhaustively evaluate practical coding strategies for OFDM and MC-CDMA. Instead, we compare the potential of the systems based on “capacity” per subcarrier. Formally, involving the data processing theorem [26], one can easily show that the Shannon capacity of OFDM and MC-CDMA are identical because the weighting operation $\boldsymbol{W}$ and the inverse code matrix $\boldsymbol{C}^{-1}$ are invertable operations. However, in order to achieve the full capacity of the link, the receiver must jointly detect MC-CDMA symbols and address the fact that the noise for the various user symbols become correlated if $\boldsymbol{W}$ uses different weights per subcarrier. However, a receiver comprised of the inverse code matrix and with a “slicer” at the outputs (as in Fig. 1) does not take advantage of this. A loss of performance occurs (relative to ideally coded OFDM) in a system that extracts N MC-CDMA symbols and processes these as if they were transmitted over an AWGN, linear time invariant, dispersion-free channel. It is reasonable to estimate the capacity per dimension of such MC-CDMA system as $1/2\log_2(1 + \zeta P_0 T_s/N_0)$.

Lee [27] proposed to estimate the capacity of the Rayleigh-fading channel as

$$\begin{aligned} C_{\text{OFDM}} &= 2\int_0^\infty f\left(\frac{E_N}{N_0}\right)\frac{1}{2}\log_2\left(1 + 2\frac{E_N}{N_0}\right)d\frac{E_N}{N_0} \\ &= 2\int_0^\infty \frac{N_0}{P_0T_s}\exp\left(-\frac{N_0}{P_0T_s}x\right)\frac{1}{2}\log_2(1+2x)\,dx. \end{aligned}$$

This can be expressed as [27] ([20, eq. 4.331.2])

$$C_{\text{OFDM}} = \frac{1}{\ln 2}\exp\left(\frac{N_0}{2P_0T_s}\right)E_1\left(\frac{N_0}{2P_0T_s}\right).$$

The exponential integral $E_n(x)$ is defined as integral from x to infinity over $z^{-n}\exp(-z)$. This expression assumes that the transmitter does not adapt its power per subcarrier to optimize

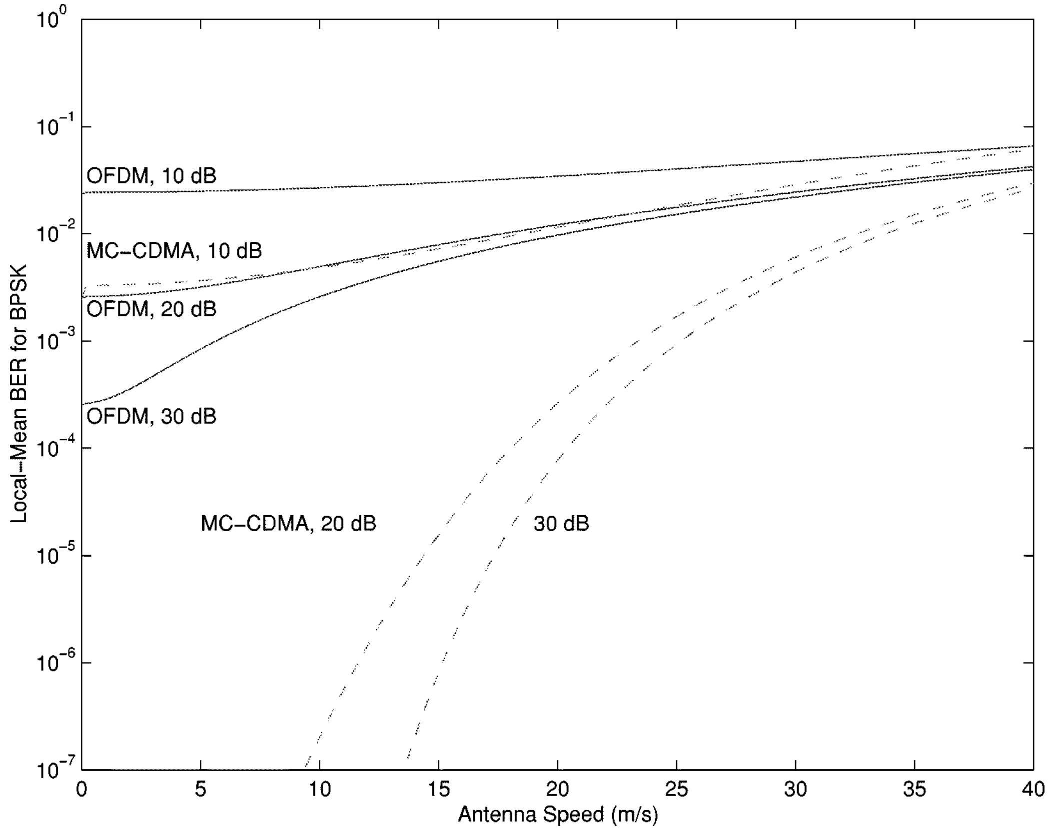

Fig. 7. Local mean BER for BPSK versus antenna speed for local mean SNR of 10, 20, and 30 dB. Comparison between MC-CDMA and uncoded OFDM.

for the instantaneous fades.[3] It was later confirmed that this capacity can be achieved in a (broadcast) system where the transmitter also cannot adapt its coding strategy based on knowledge of the individual subcarrier states [28]. It is easy to understand that OFDM can theoretically achieve the same capacity as this Rayleigh-fading channel.

For large SNR, we use $E_1(z) \cong -\gamma - \ln z$, so $C_{\rm OFDM} \cong -\gamma/(2\ln 2) + 1/2\log_2(2P_0T_s/N_0)$, thus asymptotically, OFDM on a Rayleigh-fading channel with local mean SNR P_0T_s/N_0 has approximately 0.4 bit less capacity per dimension than a nonfading channel with the SNR fixed to P_0T_s/N_0. Fig. 9 plots the capacity under Doppler spreads, using the same system parameters as Fig. 7.

VIII. Concluding Discussion

We have presented a framework that allows a theoretical estimation of the BER of MC-CDMA with a linear receiver. It includes analytical expressions for the variance of MUI and ICI in an MMSE receiver. Using this method, we found expressions for the performance of MC-CDMA, and we compared these to OFDM.

We proposed a pseudo-MMSE receiver for MC-CDMA over channels with Doppler, and analyzed its performance. BERs are better for MC-CDMA than for uncoded OFDM, though OFDM can achieve a higher performance gain from coding than MC-CDMA. A rapid deterioration of the BER is seen when antenna speeds increase, but less dramatic than reported for OFDM. Improvement is possible by implementing the true MMSE receiver settings. This appears to be computationally intensive as it requires channel estimation of many parameters and matrix inversions, but current research addresses such receivers, e.g., [33], [34].

We have also compared OFDM and MC-CDMA using Information Theoretic arguments. If we allow the constellation of the modulation to be optimized for SNR and if the number of subcarriers is very large (infinity), we found that MC-CDMA does not have an advantage over C-OFDM in terms of the theoretical channel capacity. The use of a linear receiver structure in MMSE MC-CDMA leads to a performance penalty. We concluded that for a system with many subcarriers and a channel with sufficiently large delay spread, MC-CDMA symbols see a nonfading channel. Hence, we found expressions for the performance of MC-CDMA over Rayleigh channel relative to a classic *nonfading* AWGN channel.

C-OFDM can achieve capacity only through ideal error correction decoding and channel state information. Loss of performance of linear MC-CDMA relative to OFDM is mainly due to the absence of a method to exploit correlated noise in the decision variables of the various user symbols. The performance penalty depends on the local mean SNR of the received signal. However, it becomes small for moderate SNR, say below 10 or 15 dB.

Moreover, we acknowledge that detection methods outside the scope of this paper, such as maximum-likelihood detection may achieve a performance that exceeds our results. It is also

[3]If the transmitter *can* adapt its power, Gallager's waterpooring theory applies.

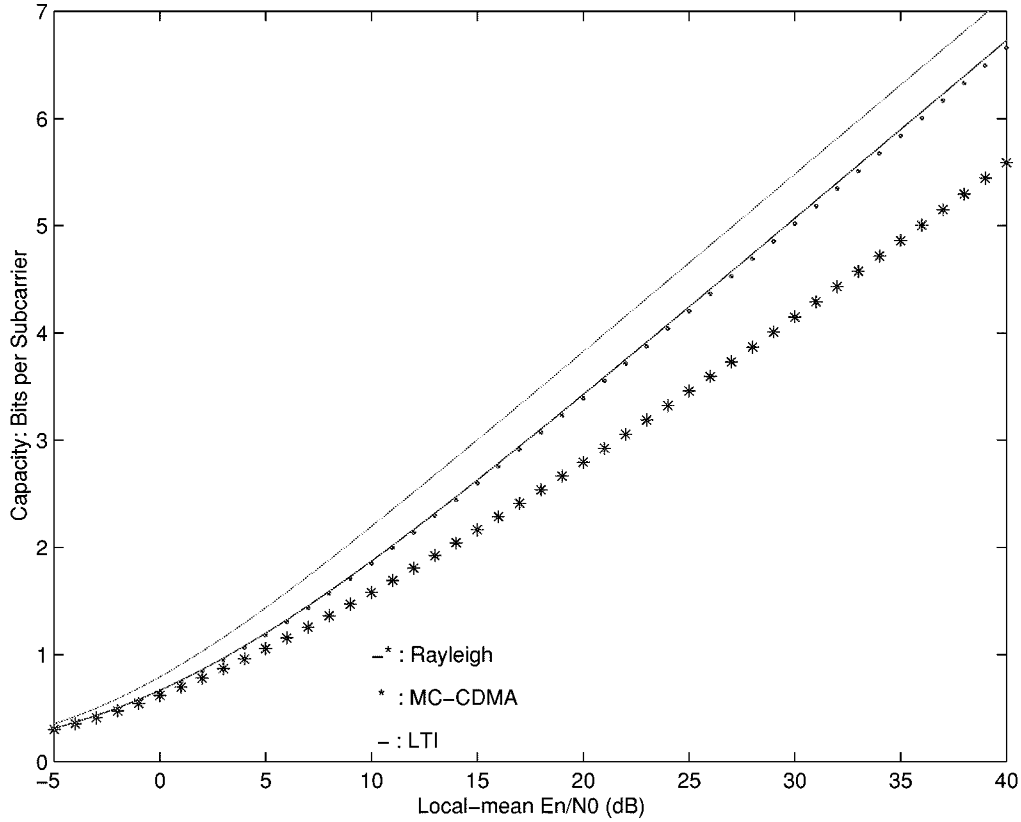

Fig. 8. Capacity per dimension versus E_N/N_0; no Doppler.

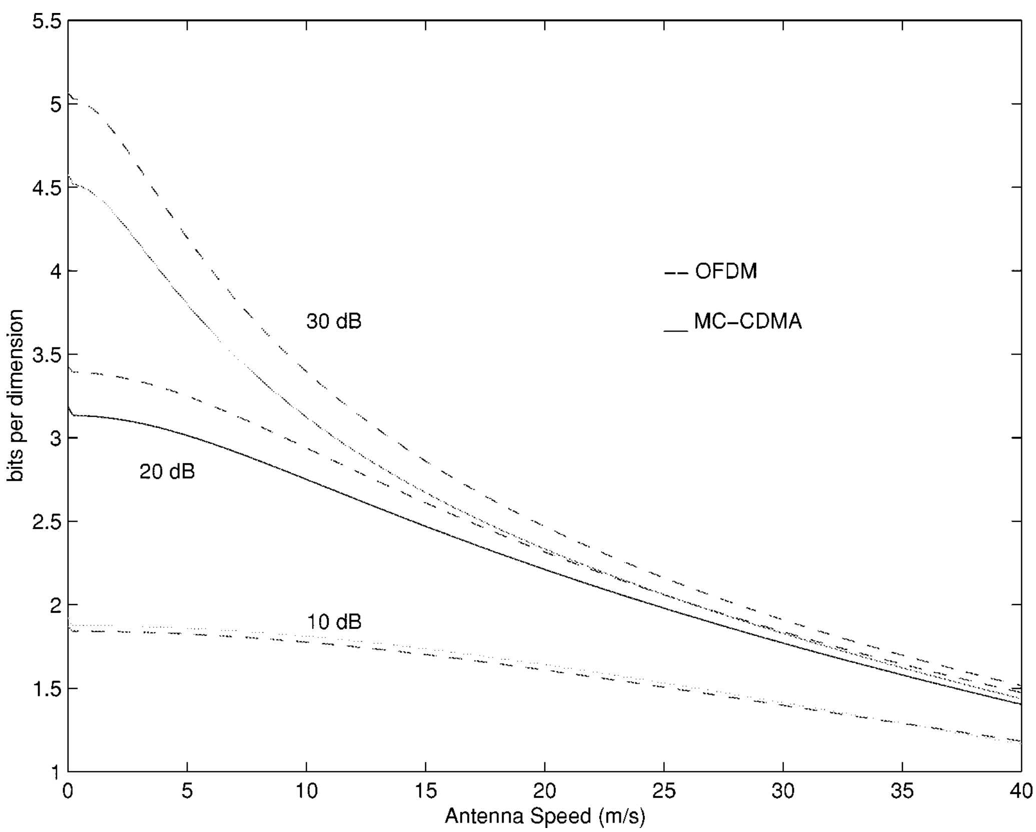

Fig. 9. Capacity in bits per dimension for OFDM and MC-CDMA versus antenna speed.

acknowledged that the above results only hold for the limiting case of a very large degree of diversity. Our model does not reveal a generic conclusion about which scheme is most favorable for a finite, fixed number of subcarriers, and a finite constellation of the modulation. With MC-CDMA, the BER vanishes with a slope that is determined by the number of independently fading subcarriers. With coded OFDM, the slope at which the BER decays is also upperbounded by a distance of the error correction code (not addressed in this paper), which typically is much smaller than N. This suggests that MC-CDMA may appear favorable in a comparison for a finite number of subcarriers and practical error correction coding schemes.

With this paper, we hope that we have contributed to a fair comparision of MC-CDMA with related modulation methods. Results indicated that for typical conditions, MC-CDMA has advantages over other modulation methods. We also identified which shortcomings prevent (linear) MC-CDMA from achieving theorectical capacity limits. The merits of MC-CDMA should be sought also in its ease of implementation as it is not substantially more complicated than uncoded OFDM. Its error correction coding can be simpler than for C-OFDM.

APPENDIX

This appendix analyzes the moments $M_{ij} = E_{\text{ch}}|\beta_{n,n}|^i |w_{n,n}|^j$, For ease of notation we denote $\beta = |\beta_{n,n}|$ and $w = |w_n| = \beta/(\beta^2 + c)$, with $c = N_0/T_s$, so

$$M_{ij} = E_{\text{ch}}[|\beta_{nn}|^i |w_{nn}|^j] = T_s^{-2} \int_0^\infty \left(\frac{\beta}{\beta^2+c}\right)^i \frac{2\beta^{j+1}}{p_0} \exp\left(-\frac{\beta^2}{p_0}\right) d\beta.$$

For M_{11}, we arrive at

$$\begin{aligned} M_{11} &= E_{\text{ch}}[\beta_{nn} w_n]^i \\ &= T_s^{-2} \int_0^\infty \left(\frac{\beta^2}{\beta^2+c}\right)^i \frac{2\beta}{p_0} \exp\left(-\frac{\beta^2}{p_0}\right) d\beta \\ M_{11} &= \left[1 - \frac{c}{p} \exp\left(\frac{c}{p}\right) \int_c^\infty \frac{1}{y} \exp\left(-\frac{y}{p}\right) dy\right] \\ M_{11} &= T_s^{-2} \left[1 - \frac{c}{p} \exp\left(\frac{c}{p}\right) E_1\left(\frac{c}{p}\right)\right]. \end{aligned}$$

In a similar fashion, M_{22} is found as

$$\begin{aligned} M_{22} &= 1 - \frac{c}{p} \exp\left(\frac{c}{p}\right) \left[2 \int_1^\infty \frac{1}{y} \exp\left(-\frac{y}{p}\right) dx \right. \\ &\qquad \left. \times \int_1^\infty \frac{1}{y^2} \exp\left(-\frac{y}{p}\right) dx\right] \\ M_{22} &= 1 - \frac{c}{p} \exp\left(\frac{c}{p}\right) \left[2E_1\left(\frac{c}{p}\right) - E_2\left(\frac{c}{p}\right)\right]. \end{aligned}$$

We use

$$E_2(z) = \exp(-z) - zE_1(z)$$

to express the MUI term

$$\begin{aligned} M_{22} - M_{11}^2 = \frac{c}{p} - \frac{c^2}{p^2} \exp\left(\frac{c}{p}\right) E_1\left(\frac{c}{p}\right) \\ - \frac{c^2}{p^2} \exp\left(\frac{2c}{p}\right) \left[E_1\left(\frac{c}{p}\right)\right]^2. \end{aligned}$$

Also, the noise enhancement, captured as M_{02}, is calculated as

$$\begin{aligned} M_{02} &= E w_n w_n^* \\ &= \frac{2}{T_s^2} \int_0^\infty \frac{\beta^2}{(\beta^2+c)^2} \frac{\beta}{p} \exp\left(\frac{-\beta^2}{p}\right) d\beta \\ M_{02} &= \frac{1}{p} \left[\left(1 + \frac{c}{p}\right) \exp\left(\frac{c}{p}\right) E_1\left(\frac{c}{p}\right) - 1\right]. \end{aligned}$$

REFERENCES

[1] S. B. Weinstein and P. M. Ebert, "Data transmission by frequency-division multiplexing using the discrete Fourier transform," *IEEE Trans. Commun. Technol.*, vol. COM-19, pp. 628–634, Oct. 1971.

[2] L. J. Cimini Jr., "Analysis and simulation of a digital mobile channel using orthogonal frequency division multiplexing," *IEEE Trans. Commun.*, vol. COM-33, pp. 665–675, July 1985.

[3] M. Alard and R. Lassalle, "Principles of modulation and channel coding for digital broadcasting for mobile receivers," *EBU Tech. Rev.*, no. 224, pp. 168–190, Aug. 1987.

[4] B. LeFloch, M. Alard, and C. Berrou, "Coded orthogonal frequency division multiplex," *Proc. IEEE*, vol. 83, pp. 982–996, June 1995.

[5] J. A. C. Bingham, "Multicarrier modulation for data transmission: An idea whose time has come," *IEEE Commun. Mag.*, vol. 28, pp. 5–14, May 1990.

[6] J. P. Linnartz and S. Hara, "Special issue on multi-carrier communications," *Wireless Personal Commun.*, vol. 2, no. 1, 2, pp. 1–7, 1995.

[7] B. LeFloch, R. Halbert-Lassalle, and D. Castelain, "Digital sound broadcasting to mobile receivers," *IEEE Trans. Consumer Electron.*, vol. 73, pp. 30–34, Aug. 1989.

[8] Mobile Reception of DVB-T, ACTS Project VALIDATE [Online]. Available: http://www.dvb.org/

[9] T. Pollet, M. V. Bladel, and M. Moeneclaey, "BER sensitivty of OFDM systems to carrier frequency offset and Wiener phase noise," *IEEE Trans. Commun.*, vol. 43, pp. 191–193, Feb. 1995.

[10] M. Russel and G. Stuber, "Terrestrial digital video broadcasting for mobile reception using OFDM," *Special Issue—MCC, Wireless Personal Commun.*, vol. 2, no. 1, 2, pp. 45–66, 1995.

[11] P. Robertson and S. Kaiser, "Effects of doppler spreads in OFDM(A) mobile radio systems," in *Proc. 56th Vehicular Technology Conf.—Fall'99*, vol. 50, Amsterdam, The Netherlands, Sept. 1999, pp. 329–333.

[12] N. Yee, J. P. Linnartz, and G. Fettweis, "Multi-carrier CDMA in indoor wireless radio networks," *Proc. IEEE PIMRC'93*, pp. 109–113, Sept. 1993.

[13] A. Chouly, A. Brajal, and S. Jourdan, "Orthogonal multicarrier techniques applied to direct sequence spread spectrum CDMA systems," in *Proc. Globecom'93*, Houston, TX, Nov./Dec. 1993, pp. 1723–1728.

[14] K. Fazel and L. Papke, "On the performance of convolutionally-coded CDMA/OFDM for mobile communication system," *Proc. IEEE PIMRC'93*, pp. 468–472, Sept. 1993.

[15] R. Prasad and S. Hara, "Overview of multicarrier CDMA," in *Proc. 1996 Int. Symp. Spread Spectrum Techniques and Applications*, Mainz, Germany, Sept. 1996, pp. 107–114.

[16] Y. Kim, S. Choi, C. You, and D. Hong, "BER computation of an MC-CDMA system with carrier frequency offset," presented at the ICCASP 99, Phoenix, AZ. CD-ROM.

[17] W. C. Jakes, *Microwave Mobile Communications*. New York: Wiley, 1978. new ed. 1994.

[18] R. H. Clarke, "A statistical theory of mobile radio reception," *Bell Syst. Tech. J.*, vol. 47, pp. 957–1000, 1968.

[19] T. Aulin, "A modified model for the fading signal at a mobile radio channel," *IEEE Trans. Veh. Tech.*, vol. VT-28, pp. 182–203, Aug. 1979.

[20] N. Yee and J. P. M. G. Linnartz, "Wiener filtering for multi-carrier CDMA," in *Proc. IEEE/ICCC Conf. Personal Indoor Mobile Radio Communications (PIMRC) and Wireless Computer Networks (WCN)*, vol. 4, The Hague, The Netherlands, Sept. 1994, pp. 1344–1347.

[21] I. S. Gradsteyn and I. M. Ryzhik, *Table of Integrals, Series and Products*. San Diego, CA: Academic, 1965.

[22] D. N. Kalofonos, M. Stojanovic, and J. G. Proakis, "On the performance of adaptive MMSE detectors for a MC-CDMA system in fast fading Rayleigh channels," in *Proc. Personal, Indoor, and Mobile Radio Conf. (PIMRC)*, Boston, MA, 1998, pp. 1309–1313.

[23] G. B. Giannakis and C. Tepedelenlioglu, "Basis expansion models and diversity techniques for blind identification and equalization of time-varying channel," *Proc. IEEE*, vol. 86, pp. 1969–1986, Oct. 1998.

[24] N. Yee and J. P. M. G. Linnartz, "Controlled equalization for MC-CDMA in Rician fading channels," in *Proc. 44th IEEE Vehicular Technology Conf.*, Stockholm, Sweden, June 1994, pp. 1665–1669.

[25] J. P. Linnartz, Ed., *Wireless Communication, the Interactive Multimedia CD-ROM*, 4th ed. Boston, MA: Kluwer, 2001.

[26] J. H. Wozencraft and I. M. Jacobs, *Principles of Communications Engineering*. New York: Wiley, 1965.

[27] W. C. Y. Lee, "Estimate of channel capacity in Rayleigh-fading environment," *IEEE Trans. Veh. Technol.*, vol. 39, pp. 187–189, Aug. 1990.

[28] E. Biglieri, J. Proakis, and S. Samai, "Fading channels: Information theoretic and communication aspects," *IEEE Trans. Inform. Technol.*, vol. 44, pp. 2619–2691, Oct. 1998.

[29] A. Gorokhov, "Blind equalization in SIMO/OFDM systems with frequency domain spreading," *IEEE Trans. Signal Processing*, vol. 48, pp. 3536–3548, Dec. 2000.

[30] Z. Wang and G. B. Giannakis, "Wireless multicarrier communications. Where fourier meets Shannon," *IEEE Signal Processing Mag.*, vol. 17, pp. 29–48, May 2000.

[31] S. Kaiser, "OFDM-CDMA versus DS-CDMA: Performance evaluation for fading channels," *Proc. IEEE Int. Conf. Communication (ICC'95)*, pp. 1722–1726, June 1995.

[32] K. Fazel and G. P. Fettweis, Eds., *Multi-Carrier Spread-Spectrum*. Dordrecht, The Netherlands: Kluwer, 1997.

[33] Y. Li, L. J. Cimini, and N. R. Sollenberger, "Robust channel estimation for OFDM systems with rapid dispersive fading channels," *IEEE Trans. Commun.*, vol. 46, pp. 902–915, July 1998.

[34] J. P. M. G. Linnartz and A. Gorokhov, "New equalization approach for OFDM over dispersive and rapidly time varying channel," in *Proc. Personal, Indoor, and Mobile Radio Conf. (PIMRC)*, London, U.K., 2000, pp. 1375–1379.

Jean-Paul M. G. Linnartz (S'85–M'87–SM'99) was born in Heerlen, The Netherlands, on September 10, 1961. He received the Ir. (M.Sc. E.E.) degree in electrical engineering (*cum laude*) from Eindhoven University of Technology, The Netherlands, in 1986 and the Ph.D. degree (*cum laude*) from Delft University of Technology, The Netherlands, in 1991.

From 1987 to 1988, he was with the Physics and Electronics Laboratory (F.E.L-T.N.O., The Hague), The Netherlands, Organization for Applied Scientific Research working on frequency planning and UHF propagation. From 1988 to 1991, he was an Assistant Professor with Delft University of Technology. From 1992 to 1993, he was an Assistant Professor with the University of California at Berkeley, where he developed and analyzed random multiple access schemes for multipath fading channels and introduced multicarrier cdmA. In 1994, he was with Delft University of Technology as an Associate Professor. In 1995, he joined Philips Electronics, Eindhoven, The Netherlands, to initiate a research activity on conditional access for multimedia content, copy control, and security at the Natuurkundig Laboratorium, Natuurkundig (physics) Laboratorium, Eindhoven, The Netherlands. Later, he became Principal Scientist there and he is now Department Head. His group actively participates in various standardization fora, in particular for secure audio and video formats and for protection of prepackaged (DVD) and broadcast content. The group developed the Millennium watermarking system for DVD content protection and broadcast monitoring. Since 1999, he has had a TechTalk Internet radio station featuring tutorials on wireless communication. During his studies, he was a freelance program host for radio stations in Belgium and The Netherlands. He participated in the organization of conferences in radio communication, networks, subliminal communication, watermarking, and signal processing. He has ten patents in the field of electronic watermarking and copy protection. He is founding Editor-in-Chief of *Wireless Communication, The Interactive Multimedia CD-ROM* and he authored the monograph, "Narrowband land-mobile radio networks," and various book chapters.

Dr. Linnartz received the 1991 NERG Veder Prize for his work on random access in wireless networks. He has been an invited speaker and a session and panel chairmen for conferences on wireless communication, signal processing, and security.